



## Stochastic acceleration in the heliosheath: effect on anomalous cosmic ray spectra

H. Moraal<sup>1</sup>, R.A. Caballero-Lopez<sup>2</sup>, V. Ptuskin<sup>3</sup>

<sup>1</sup>Unit for Space Physics, North-West University, Potchefstroom, 2520, South Africa

<sup>2</sup>Instituto de Geofísica, UNAM, 04510, México

<sup>3</sup>IPST, University of Maryland, College Park, MD, 20742, USA

harm.moraal@nwu.ac.za

**Abstract:** It is generally accepted that shock acceleration by the solar wind termination shock is the primary process that establishes the anomalous cosmic ray component. There may, however, be secondary processes that produce and/or accelerate these particles. In this paper we point out that stochastic acceleration in the outer regions of the heliosheath is such a process.

### Introduction

When Voyager 1 crossed the termination shock of the heliosphere in December 2004, the observed spectra of the anomalous cosmic ray (ACR) component were not of the form as expected from standard applications of the first order Fermi or shock acceleration process [1]. It was subsequently shown that temporal effects probably dominated the spectral shape [2], [3]. However, the investigation of these spectra alerted us to the fact that other mechanisms may contribute to the production and acceleration of ACRs in the outer heliosphere. In [4] we pointed out for the first time that second order Fermi (or stochastic) acceleration in the outer heliosheath is such a mechanism. This acceleration is generally unimportant in the supersonic solar wind, but we showed that it may be a viable process in the outer regions of the heliosheath where the turbulence levels are much higher, due to the slow-down of the solar wind. Here we repeat some of those calculations and we point out what the general features of this stochastic acceleration are.

### The cosmic ray transport equation

To study these acceleration and modulation processes we consider numerical solutions of the cosmic ray transport equation (TPE) for the evo-

lution of the cosmic-ray distribution function,  $f$ , in terms of momentum  $p$ :

$$\frac{\partial f}{\partial t} + \mathbf{V} \cdot \nabla f - \nabla \cdot (\kappa \cdot \nabla f) - \frac{\partial f}{\partial \ln p} - \frac{1}{p^2} \frac{\partial}{\partial p} (p^2 D \frac{\partial f}{\partial p}) = Q \quad (1)$$

Here  $\mathbf{V}$  is the solar wind velocity and  $\kappa(\mathbf{r}, P, t)$  the diffusion tensor, with elements  $\kappa_{\parallel}$  and  $\kappa_{\perp}$  for scattering along and perpendicular to the HMF,  $\mathbf{B}$ , together with an antisymmetric coefficient  $\kappa_T(\mathbf{r}, P, t) = \beta P / (3B)$  that incorporates gradient, curvature, neutral sheet, and shock drifts. The latitudinal and radial components of these coefficients are given by  $\kappa_{rr} = \kappa_{\parallel} \cos^2 \psi + \kappa_{\perp} \sin^2 \psi$  and  $\kappa_{\theta\theta} = \kappa_{\perp}$ . The HMF is taken as the standard Parker spiral field with a value 5 nT at Earth. The solar wind termination shock (SWTS), with compression ratio  $s$ , is put at  $r_s = 90$  AU, with the outer boundary,  $r_b$ , corresponding to the heliopause, at 180 AU. Inside the shock  $V = 400$  km s<sup>-1</sup> while in the heliosheath  $V = (400/s)(r_s/r)^2$  km s<sup>-1</sup>. We let it increase with a factor of 2 between latitudes of 20° and 30°, which is representative of solar minimum conditions.

The last term on the left of (1) describes diffusion in momentum space. In the supersonic solar wind it is small compared to adiabatic energy losses and it is usually neglected. In the following sections it is pointed out, however, that it may be significant in the heliosheath.

### Stochastic acceleration in the solar wind

Stochastic acceleration is unimportant inside the termination shock. The Alfvén speed is  $V_A = B/\sqrt{\mu_0\rho}$ , with  $\rho$  the solar wind density. Using the Parker field values above, this velocity at 1 AU is  $V_A \approx 40$  km/s. For  $r \gg 1$  AU, the Parker field falls off  $\propto r^{-1}$ , and since  $\rho \propto r^{-2}$ ,  $V_A$  is independent of  $r$ . According to [6] the diffusion coefficient for stochastic acceleration is  $D = p^2 V_A^2 / 9\kappa_{\parallel}$ . The time scale for this acceleration is then  $\tau_{\text{stoch}} \sim p^2/D = 9 \kappa_{\parallel}/V_A^2$ . A typical value for the parallel diffusion coefficient at Earth, that provides a reasonable fit for modulation observations, is  $\kappa_{\parallel} = 6 \times 10^{22} \beta P$  (GV)  $\text{cm}^2 \text{s}^{-1}$ . Thus, this time-scale for stochastic acceleration becomes  $\tau_{\text{stoch}} \sim 4 \times 10^5 \beta P$  (GV) days. To be a viable process, this time must be comparable to other time scales in (1). The time for propagation out to the SWTS at  $r_s = 90$  AU is  $\tau_{\text{conv}} \approx 390$  days. That for acceleration by the SWTS to a power law is  $\tau_{\text{shock}} \sim \kappa/V^2 \approx 430 \beta P$  (GV) days. (We note that perpendicular diffusion is the dominant process here, and from our experience with solutions of (1) the value of this coefficient at 90 AU should be of the same order of magnitude as  $\kappa_{\parallel}$  at 1 AU; hence, we have used that value). This means that for typical 80 MeV protons, for which  $\beta P = 0.15$  GV, the ordering of time scales is

$$\tau_{\text{shock}} \approx 64 < \tau_{\text{conv}} \approx 390 < \tau_{\text{stoch}} \approx 60\,000 \text{ days} \quad (2)$$

This shows that in the supersonic solar wind the stochastic process is much too slow to be effective.

### Stochastic acceleration in the heliosheath

The situation is quite different in the heliosheath. If  $V_0$  and  $B_0$  are the wind and HMF values immediately inside the shock, their profile in the heliosheath is  $V = (V_0/s)(r_s/r)^2$  for incompressible subsonic flow, and  $B = B_0 s(r/r_s)$  if the Parker field is maintained. Thus the downstream Alfvén speed is  $V_A = 40 (r/r_s) s^{1/2}$  km/s. If the diffusion coefficients in the heliosheath scale  $\propto B^{-1}$ , then it follows from the above that the coefficient for stochastic acceleration in the heliosheath is given by

$$D_{\text{heliosheath}} = s^2 (r/r_s)^3 D_{\text{solar wind}} \quad (3)$$

For  $r_s = 90$  AU and  $r_b = 180$  AU the convection time in the heliosheath is  $\tau_{\text{conv}} = \int dr/V$ . Using the  $r^{-2}$  dependence of  $V$  as above, this gives  $\tau_{\text{conv}} \approx 3600$  days. This is almost an order of magnitude longer than the convection time from the sun to the SWTS. On the other hand, it follows from the same calculation as above that for 80 MeV/n protons  $\tau_{\text{stoch}} \approx 230$  days at  $r_b = 180$  AU.

This acceleration time is so fast in comparison with  $\tau_{\text{conv}}$  and  $\tau_{\text{shock}}$  that stochastic acceleration in the outer regions of the heliosheath seems a quite viable process to contribute to the acceleration of low-energy particles to ACRs. The physical reason is that the turbulent magnetic fields accumulate in the outer regions of the heliosheath, and have ample time to accelerate the cosmic rays there.

### Model solutions

Based on the above arguments we show three solutions of the transport equation, similar to those in [4], to demonstrate the effect of this stochastic acceleration. In this demonstration we are not concerned with the galactic cosmic ray component, and therefore take the intensity on the outer boundary at  $r_b = 180$  AU equal to zero. In addition to the parameters mentioned in the previous two paragraphs, we also specify a monoenergetic source,  $Q$ , of low-energy particles at 50 KeV/n, which can be accelerated by both the shock and the stochastic process to higher energies. A moderate shock, with compression ratio  $s = 3$ , is placed at  $r_s = 90$  AU. Solutions are only shown for the  $qA < 0$  drift case, as it is in the current epoch until the next solar maximum. The main stochastic acceleration effects are similar in the  $qA > 0$  and no-drift solutions. Further details of the model are given in [5].

Figure 1 shows the spectra of ACR  $\text{He}^+$  produced by these solutions. Panel A is a reference solution that does not contain stochastic acceleration, and therefore the ACR spectra are entirely produced by the shock. Notice that the spectral shape at 95 AU is near to the expected form  $j_T \propto T^{-1.25}$  (for  $s = 3$ ) up to  $\approx 20$  MeV/n, whereafter it rolls over due to shock curvature effects. This same spectral shape is approximately maintained throughout the heliosheath, as shown by the spectrum at 150 AU.

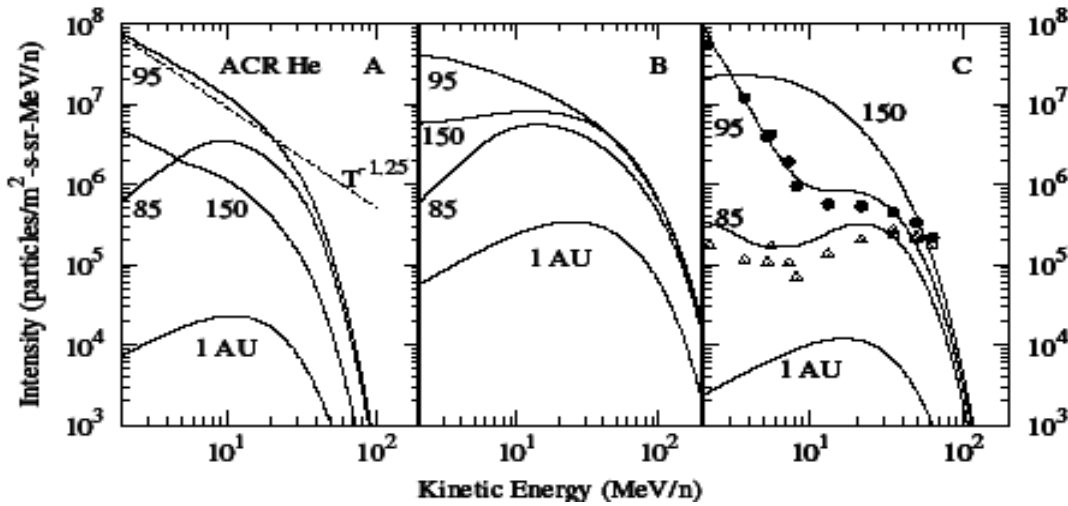


Figure 1: ACR  $\text{He}^+$  spectra, at radial distances as shown and in the ecliptic plane, produced by three different acceleration models. Panel A is the standard shock acceleration solution for  $s = 3$  with no stochastic acceleration. The dashed line on the 95 AU spectrum is the shape expected on the shock (at 90 AU) if the shock were plane. In panel B stochastic acceleration is added according to the values calculated from (3). In Panel C this stochastic acceleration is concentrated in the outer regions of the heliosheath, while a weaker shock ( $s = 1.5$ ) is chosen. Observations are from V1 (full) and V2 (open) on 16-23 Jan. 2005

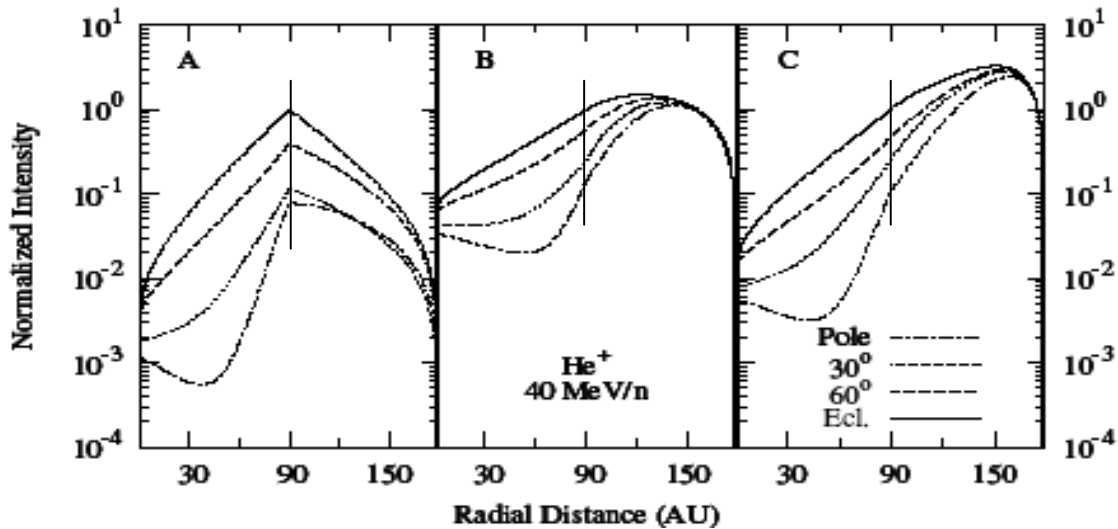


Figure 2: Radial intensity profiles for 40 MeV/n ACR  $\text{He}^+$  for the same solutions that produce the spectra in Figure 1.

Inside the shock, at 85 and 1 AU, the standard modulation effects are clear.

Figure 2A shows the radial intensity distribution for 40 MeV/n ACR  $\text{He}^+$  for the same parameters, at heliolatitudes  $0^\circ$ ,  $30^\circ$ ,  $60^\circ$ , and  $90^\circ$ . The intensi-

ties are normalized to 1 for  $r = r_s$  and in the ecliptic plane. These four profiles show the well-known negative latitudinal gradients in the  $qA < 0$  drift state.

Figures 1B and 2B show the solutions for the case when stochastic acceleration is included. The parameters used are those leading up to (3). This changes both the spectra and the radial intensity distributions significantly. The most important change is that the spectra in Figure 1B extend to  $\sim 5$  times higher energy than in Figure 1A before they roll over. This is due to the shock-accelerated particles of the previous model (Panels A) that are convected downstream and re-accelerated significantly by the stochastic process. This process is most effective in the outer heliosheath due to the  $r^3$  dependence of the efficiency in (3), and it leads to the very flat spectrum at 150 AU. These flatter spectra, in turn, lead to much smaller radial gradients as can be seen when Panel 2B is compared to 2A. Furthermore, the local maximum in the intensity at the SWTS at  $r_s = 90$  AU is now absent because the stochastic process, and not the shock, is the dominant source of these high-energy particles.

It is clear from Panels A and B in Figures 1 and 2 that the combination of two such independent acceleration processes can lead to a very wide range of spectral shapes and spatial intensity distributions. Alternatively, a given observation can be explained with an equally wide range of parameters. This parameter space must be narrowed by further study of these processes, especially as they pertain to the uncertain regions of the outer heliosheath.

A case in point is shown in Figures 1C and 2C. These panels contain the same solutions as in Figures 1B and 2B, except that the coefficient  $D$  for stochastic acceleration is multiplied by  $(r/r_b)^6$  to concentrate this process almost entirely in the outer heliosheath, and a weak shock, with  $s = 1.5$ , is taken. These solutions provide an adequate fit for the spectral shape observed from 16 to 23 January 2005, just after V1 crossed into the heliosheath, with V2 still in the solar wind. In this case the 95 AU spectrum at  $T < 10$  MeV/n is mainly produced by the shock, while that at  $T > 10$  MeV/n now consists mainly of particles that were accelerated far out, at  $r \approx 150 - 170$  AU, and then modulated on their way in. It is this modulation that causes the inflection in the 95 AU spectrum.

Note that the solutions of (1) are fully self-consistent, i.e. the only free parameter is the absolute source strength,  $Q$ , at 0.05 MeV/n. The spectral forms, specifically the cutoffs, are determined naturally by the various scalings, and are not added artificially or post-hoc.

We emphasize that this interpretation of these particular two spectra is not necessary or exclusive, in particular due to the studies of [2] and [3], that have shown that the shape is probably due to temporal effects passing by the spacecraft. This current fit merely demonstrates the wide range of possible spectral shapes that can result if there is more than one ACR source, in particular if they are situated in different regions of the heliosphere. Notice in particular that two very different physical models such as in panels A and C of the figures, lead to very similar radial spatial distributions inside the shock (but entirely different outside it).

### Conclusions

Stochastic acceleration in the outer regions of the heliosheath is probably a viable process that, amongst several others, may make a significant contribution to cosmic ray intensities in the heliosphere. Since it occurs with greatest efficiency at positions far removed from the site of shock acceleration at the SWTS, the combined processes can lead to quite complex spectral shapes throughout the heliosphere.

### References

- [1] Stone, E.C., Cummings, A.C., McDonald, F.B., Heikkila, B.C., et al., *Science*, 309, 2017, 2005.
- [2] Caballero-Lopez, R.A., Moraal, H., McDonald, F.B., *Proc. 30<sup>th</sup> Int. Cosmic Ray Conf*, paper 0055, 2007.
- [3] Florinsi, V., and Zank, G.P., *Geophys. Res. Lett.* 33, L15110, doi:10.1029/2006GL026371, 2006.
- [4] Moraal, H., Caballero-Lopez, R.A., McCracken, K.G., McDonald, F.B., Mewaldt, R.A., Ptuskin, V., Wiedenbeck, M.E., *AIP Conf. Proc.* 858, 219, 2006.
- [5] Steenberg, C.D., & Moraal, H., *J. Geophys. Res.*, 104, 24879, 1999.
- [6] Ptuskin, V., Moskalenko, I.V., Jones, F.C., Strong, et al., *Ap. J.* 642, 902, 2006.